Composite Structures 337 (2024) 118091

Contents lists available at ScienceDirect

Composite Structures

journal homepage: www.elsevier.com/locate/compstruct

A novel ductile connection for FRP pultruded beam-to-column assemblies

Francesco Ascione [a,*], Mario D'Aniello [b], Luciano Feo [a], Luigi Granata [a], Raffaele Landolfo [b]

[a] Department of Civil Engineering, University of Salerno, Italy
[b] Department of Structures for Engineering and Architecture, University of Naples "Federico II", Italy

ARTICLE INFO

Keywords:
FRP
Adhesive
Steel
Ductile behaviour
Experimental tests

ABSTRACT

The resistance, stiffness and ductility of the joints between Fibre Reinforced Polymer (FRP) members play a key role in ensuring the required structural performance of pultruded composite frames. Both bonded and bolted joints are characterised by poor mechanical performance due to brittle failure and low resistance respectively. Hybrid joints are stronger and more ductile, but are still affected by some criticisms such as (i) non-repairability, (ii) the presence of holes in the fibre-reinforced material, (iii) the difficulty of assembling a transverse beam into the joint, which is typically required for real 3D systems. To overcome such limitations, a novel ductile connection has been developed by combining ductile steel elements bonded to FRP members. The steel elements are bolted together and are designed to be weaker than the FRP profiles and adhesive. Experimental tests on beam-column assemblies have been carried out and the test results have shown that the investigated hybrid connection is characterised by adequate stiffness, resistance and high ductility. The damage is concentrated in the bolted steel elements, which can be easily replaced, confirming the repairability of the assembly.

1. Introduction

The connections between Fibre Reinforced Polymer (FRP) members play a key role in ensuring the required structural performance. Either premature or brittle failure of the connections can lead to the disproportionate collapse of the entire structural system. On the other hand, if the connections are excessively weaker than the connected members, the structural efficiency will be compromised due to the inefficient use of the connected members. Therefore, the connections should provide sufficient resistance to effectively utilise the mechanical properties of the FRP profiles [1].

The connections between FRPs are typically characterised by structural and mechanical criticisms, mainly due to the brittle and anisotropic properties of the material [2,3]. Both bolted and bonded joints have been extensively studied. Previously, bolted joints were developed and adapted based on design criteria close to those of steel joints [4–18]. In the last decade, adhesive joints have been studied and are becoming more popular due to their superior performance [19–23]. In fact, the adhesive technology allows both the minimisation of the stress concentration between the mechanical components making up the bonded assembly and the uniform distribution of loads and stresses over the entire surface concerned, thus resulting in a greater resistance to bending and vibrational effects.

In addition, the resin can be perfectly adapted and compatible with the shapes and characteristics of the parts to be bonded, and it guarantees the continuity of the fibres. Compared to other joining methods, it allows a reduction in the number of components (screws, nails, etc.) and consequently in the weight.

On the other hand, adhesive technology has further design and mechanical disadvantages compared to bolted joints. Bonded joints typically exhibit brittle failure modes that start in the adhesive layer. Such a limited deformation capacity is highly undesirable for earthquake resistance. In addition, these joints are also prone to loss of strength and stiffness at elevated temperatures and in aggressive environments. In addition, it is necessary to guarantee both adequate surface preparation and setting times, which vary according to the type of adhesive.

In the field of building construction, the greatest efforts of most researchers have been concentrated on developing a type of joint that simultaneously offers an adequate level of ductility and resistance. Within this framework, hybrid joints can be a viable solution that conveniently combines fibre-reinforced material and steel [24–29], where plastic deformations in the steel elements are promoted to prevent the failure of the brittle connected elements.

These considerations motivated the study summarised in this article, which aimed to develop a patented ductile joint for FRP pultruded beam-column assemblies. The proposed system is a hybrid joint in which

* Corresponding author.
E-mail address: fascione@unisa.it (F. Ascione).

https://doi.org/10.1016/j.compstruct.2024.118091
Received 21 November 2023; Received in revised form 14 February 2024; Accepted 31 March 2024
Available online 3 April 2024

the ductile component is a built-up mild steel connection properly bonded to FRP members. The joint is specifically made up of different sub-components designed to behave elastically and only one of them is designed as a structural fuse, namely weaker than the others as well as the connected FRP members. This type of assembly guarantees (i) fibre continuity by bonding the FRPs to ductile elements where the plastic deformations are concentrated, (ii) ductility and (iii) easy reparability.

The study supporting the development of the proposed joint is summarised in this paper, which is divided into four main parts. First, a brief review of the state of the art is presented and discussed to highlight the criticisms of the main types of joints previously studied and more commonly used. The second part focuses on the description of the proposed joint and the relevant design criteria. The third part presents the experimental programme, while the last part discusses the main results and findings of the experimental study.

2. Review of the state of the art

2.1. Generality

Three types of technology have been investigated and used to connect FRP members, namely (i) bolting, (ii) bonding and (iii) hybrid (i.e. a combination of bolting and bonding) connections. In contrast to steel and reinforced concrete systems, the connections between FRP members in primary structures are generally weaker than the connected members (i.e. "under-resistant"). A brief review of the relevant state of the art is summarised below with the aim of highlighting the advantages and disadvantages of the most common types of connections.

2.2. Bolted connections

Bank et al [4,5] carried out a pioneering experimental study of four types of bolted connections between open pultruded profiles. The connections were mainly designed according to the rules of steel structures adapted to FRPs. Due to the anisotropy and brittle behaviour of FRPs, these connections were detailed with a large number of stiffening elements to prevent premature local failure. These authors started with a single stiffener (angle) between the beam web and the column flange, to continue with the addition of a seat angle between the column flange and the lower beam flange, or to add only seat angles between the column flange and both the upper and lower beam flanges, or to add all the previously described stiffeners. The best-performing connection in terms of resistance and stiffness was the last one.

In order to simplify and speed up the assembly between FRP members, as well as to improve the mechanical performance of the connections, the so-called "universal connector" system was developed by Mosallam et al [6,7]. This system consists of two classical seat angles reinforced by diagonals at the edges, which are bolted to the beam and column by means of through-bolts. The experimental tests confirmed the beneficial effects of this type of stiffening on the resistance of the joint, despite the localisation of damage in the flanges of the connected members due to the bearing pressure exerted by the connectors [7].

The same authors modified the shape of the haunched stiffeners to allow them to be wrapped with a GFRP sheet, resulting in the so-called "wrapped connector" [8].

The experimental tests showed that the connections with wrapped connectors could have a higher stiffness than the bolted ones, although their resistance was 30 % lower. The technological feasibility of their joints was also discussed, concluding that the wrapped system is more convenient in terms of ease of application.

In order to enhance the rigidity and resistance of the beam-to-column joints, cuff connections were designed to enhance the performance of beam-column joints between both open and closed section profiles [9,10]. The idealized cuff connection consisted of a monolithic steel T element where the FRP members are inserted in and bonded to the steel cuff. The tests performed confirmed the substantial increase of the stiffness and resistance of such connections as respect to those with bolted haunches, about 90 % and 300 % more, respectively.

Qureshi and Mottram [11–13] tested pultruded beams-to-column joints equipped with bolted steel cleats connecting the beam webs to the column (the two beams were aligned), concluding that these connections may satisfy the requirements of the Eurocomp design code [14].

Martins et al. [15] studied an innovative blind beam-to-column bolted connection system for GFRP tubes, comprising ad-hoc built-up steel devices to be inserted into the GFRP hollow sections and bolted together. In particular, four different configurations were tested, namely one bolt per web (i), two bolts per flange and short end distance (ii), four bolts per flange (iii), two bolts per flange and a longer end distance (iv). They observed that the maximum rotational stiffness was provided by the (iii) configuration while the maximum failure load by the (iv) configuration.

Russo [16] studied the so-called multi-bolted (MB) and high multi-bolted (HMB) connections. This study underlines the limits of accuracy of the existing design formulas for FRP connections. Furthermore, the tests showed that net-tension and cleavage failure modes are prevented while mixed bearing and shear-out collapse modes occur in vertical and horizontal bolt rows depending on the load orientation.

Luo et al. [17] presented an innovative nodal joint system with thin-walled steel sleeve and plate for development of latticed shell structures using hollow section glass fibre reinforced polymer (GFRP) members. In the proposed system, the GFRP members were connected to a steel gusset-plate by through bolts in vertical and horizontal directions.

The first failure was bottom web-flange separation of the GFRP end section because of the bottom flange of GFRP was pushed downwards by the inner steel tube during bending deformation.

This type of failure was immediately followed by longitudinal cracks on the top flange of the GFRP section because the GFRP top flange pushed upwards at the contact region between the GFRP hollow and the end section of the inner steel tube. Subsequently, ultimate failure occurred due to the excessive web-flange separation leading to a significant loss of load-carrying capacity.

More recently, the behaviour of a stainless steel cuff beam-to-column bolted connection has been studied by Martins et al for tubular profiles [18] and I-section members [19] in order to achieve higher ductility and corrosion resistance. In particular, four different beam-to-column connection series were adopted for both joints, obtained by varying only the length and thickness of the sleeve. The experimental campaign, which included (i) monotonic tests for all the series and (ii) cyclic tests for the series with the best performance in the monotonic tests, showed that the greater sleeve thickness the higher initial stiffness and strength, even though the lower ductility. In addition, the results indicated that the sleeve connection is more efficient for joining tubular sections than open sections such as I-sections. Therefore, the same authors experimentally studied a different solution for beam-to-column bolted connections between GFRP I-beams [20], using stainless steel cleats, modifying their position and thickness, and using column reinforcements. The series of specimens that showed the best overall mechanical behaviour consisted of 6 mm thick flange cleats with two rows of bolts and column reinforcements, with the best balance between initial stiffness and non-linear deformation capacity. In addition, these authors developed analytical predictions of the stiffness and strength of the reinforced joint [21].

The last study was presented by Ferrara et al [22] about the mechanical characterization of a screw connection realized with steel plates used for defining innovative technological buildings with low environmental impact realized by fibre-reinforced materials. For this purpose, two different configurations, a beam to-column joint and a whole portal frame, were tested to evaluate the resistance and the stiffness of the connection. In addition, the beam-to-column element was also subjected to cyclic loads to assess the joint energy dissipation capacity. The resistance value was found, as expected, with reference to

the bearing failure that occurs between bolts and steel plates. All in all, with respect to mechanical aspects, the study confirms the suitability of pultrude FRP element assemblies for modular building applications.

2.3. Bonded connections

In 2005 Singamsethi et al. [23] modified, designed, and fabricated the cuff connection previously introduced by Smith at al. [9,10]. The cuff was fabricated using a vacuum-assisted resin transfer moulding (VARTM) process where the cuff was made of steel. Two different number of layers were adopted:13 and 15 layers. the cuff was conceived for box elements to be inserted inside it by adhesive.

Carrion et al. [24] continued the work by Smith et al. [9,10] and Singamsethi et al. [23], presenting the results of monotonic and cyclic tests in order to investigate the performance of different variations of the cuff connection produced using the VARTM process. Twelve frames were tested, evaluating their behaviour from the standpoints of stiffness and strength. Monolithic cuff connections of moderate thickness were capable of developing the flexural capacity of a pultruded FRP box beam (with proper detailing), and the cuffs themselves exhibited somewhat ductile failure modes upon reaching their maximum load.

A pioneer experimental study on the behaviour of adhesively beam-to-column moment resisting connections under static load was carried out by Ascione et al. [25], which tested four assemblies with I-profiles for both beam and column. In all cases, the beam flanges and web were epoxy bonded to the column through angle cleats, varying the location of the connection with respect to the free end of the column and the column strengthening method. The angles were used to connect both the flanges and the web of the beam to the flange of the column. These tests showed that fully bonded connections can exhibit ultimate resistances similar to those provided by bolted connections, although poor ductility due to the brittle failure of the adhesion.

More recently, Razaqpur et al. [26] proposed a new adhesive beam-to-column connection which comprises a square GFRP hollow column that is connected to a built-up beam made of two GFRP U-profiles by means of either epoxy or steel bolts. The results of both quasi-static and cyclic tests showed that this type of connection may exhibit a significant increase of resistance and stiffness compared to bonded connections previously discussed [25]. In addition, the adhesive connection exhibited resistance and stiffness greater than those of the companion bolted connections of about 82 % and 380 %, respectively. Although these connections can provide a flexural resistance in the range of 20 % to 30 % of the bending resistance of the connected beams, the ductility is rather poor due to their brittle failure.

In addition, all examined types of bonded connections are feasible for 2D planar moment frames, because transverse beams cannot be easily connected to the nodal element, thus potentially limiting the field of practical applications.

It can be observed that the adhesive connections exhibit significantly higher resistance and stiffness than the companion bolted connections. In fact, the average failure moment of the adhesive connections is nearly twice that of the bolted connections and their average stiffness is twice greater than the values of the corresponding bolted connections.

Continuing the previous experimental results, those Authors tested the same adhesive connection pointing their attention to the influence of several parameters, such as the extension of the bonded area, the load condition, and hygro-thermal aging on the global mechanical response of beam-to-column adhesive joints [27]. These test results showed that the variation of the bonded area influences the resistance but not the stiffness of the connections while the hygro-thermal aging influences mainly the stiffness.

2.4. Hybrid connections

Hybrid connections combine both bonded and bolted components. In 2016, a novel bonded sleeve connection between GFRP hollow beams and steel columns was presented by Wu et al. [28,29]. The GFRP beam was either bonded to a steel sleeve (the latter connected to the columns by means of a bolted steel end-plate) or directly fastened by steel bolts and connected to the columns through steel angles. The tests showed that the thickness of the steel components (e.g., end-plate and angles) highly influences the initial stiffness and the flexural resistance of the connections.

Zhang et al. [30] developed an improvement of the previous [28,29] bonded sleeve connections. The differences with respect to the previous connection are summarized as follows: (i) both beam and columns are box sections; (ii) the sleeve connector is obtained by welding a steel tube to a steel endplate. The steel tube is also inserted into and adhesively bonded with the GFRP beam end, and the end-plate is connected to the GFRP column using through-bolts. Four beam-to-column specimens with different bond widths (80 mm and 160 mm) between the GFRP beam and steel tube and different numbers of bolts (4 or 8 bolts) were tested.

Comparison between the results of two tests with different bonding widths suggested that the specimens with a bond width of 160 mm had considerably higher moment capacity (about 35 %) than those with a bond width of 80 mm, with failure initiations shifted from cohesive failure to yielding of the steel end-plate.

In 2019, an experimental and numerical study on the bending performance of splice connections for tubular FRP members was carried out by Qiu et al. [31], which consisted of steel bolted flange joints between two tubular steel-FRP bonded sleeves. The experimental response of these connections was satisfactory thanks to the excellent ductility provided by the yielding of the steel flanges.

In 2021 another type of hybrid connection for pultruded glass fibre reinforced polymer (GFRP) frame was tested under monotonic and cyclic loading by Feng et al. [32]. The geometry of the connection was very similar to that of Razaqpur at al. [26] but the column was made of two box profiles that were bonded to each other. This type of connection exhibited a very promising response showing a quasi-plastic behaviour, even though the limited ductility. In fact, the sequence of damage was characterized by the initial failure of the adhesive that was followed by GFRP failure at bolt holes. The resistance of the connection was that one of the adhesive layers, while bolts avoided the collapse of the system.

As discussed previously, FRP joints suffer from the problem of transfer of high shear loads with bolted connections due to the low pin-bearing resistance of the material and to the elastic-brittle behavior which does not allow significant plastic redistribution of stresses between the different bolt rows. In order to overcome these issues a slip-critical connection with steel and PFRP plates was examined by Feo et al. [33]. Slip-critical connections, currently, are not allowed by national and international codes dealing with pultruded structures also due to the limited knowledge that has been achieved up to now by the scientific community. In order to try to fill this knowledge gap, experimental tests on specimens realized with mild-steel plates and PFRP plates extracted from web and flanges of a structural profile, were carried out. All the tested connections exhibited a behavior characterized by the attainment of a slip critical load, followed, after the achievement of the contact of the bolt shank with the hole, by the activation of and extra resistance related to the pin-bearing response of the connection. This behavior provides a response characterized by a pseudo yielding and pseudo-ductility which, considered the brittle behavior of pultruded elements, may be seen as beneficial effects for the global behavior of the connection.

3. The proposed ductile connection

The proposed joint is designed to bond FRP pultruded profiles to steel elements to maintain the continuity of the fibres. The steel elements are bolted to other steel components which are designed to be weaker than the bond strength in order to ensure a ductile response. This arrangement makes it possible to optimise the mechanical response of the

materials used and to maintain the typical construction technology of FRP and steel structures.

Fig. 1 shows the geometrical features of the proposed connection, which consists of (1) a "nodal element" made of a steel section welded to a top and bottom end plate (see the red I-section, but a hollow section is also feasible); (2) a steel sleeve (see the blue element) arranged with an end plate to be bolted to the nodal element and bonded to the FRP column (i.e, (3) a steel channel (the green element) designed as the weaker component of the assembly; (4) a steel T-joint (the purple element) bolted to the steel channel and bonded to the FRP beam (i.e. the two yellow C-profiles). The geometry of the beam, column and nodal element can vary according to the design requirements and construction needs, while the concept of the other components of the connection can remain the same. In fact, the green element is the structural fuse, designed as a sacrificial element that guarantees the ductility, resistance and rigidity of the beam-column assembly, but it can also be easily disassembled by unscrewing the bolts and replacing them with a new one. In addition, this type of connection makes it easy to create internal, corner and 3D beam-to-column assemblies, as these steel channels can be bolted to the four sides of the node element. In this case, a hollow steel section should be used instead of an I-section to achieve the same stiffness in all directions (see Fig. 2).

It is also worth noting that the proposed connection has been recently patented by the authors through the University of Salerno [34].

4. Experimental program

4.1. Generality

The aim of the testing program was to investigate the influence of the following parameters on the flexural response of the proposed connection:

- the bonding width (L_α) between the GFRP built-up beam and the steel T-Stub. As depicted in Fig. 6, two different values were adopted: 150 mm and 220 mm. These values were selected in order to have a bonding width of about two (i.e., 150 mm) and three (i.e., 220 mm) times bigger than the minimum required adhesive width b_{eff}, which is about 70 mm on the basis of Eq. (3);

- the pitch of the bolts (d_γ) connecting the previous steel T-Stub to the fuse. As depicted in Fig. 6 two different values were considered: 60 mm and 80 mm;
- the thickness of the web of the fuse (t_β), which was varied as follows: 2 mm, 3 mm, 4 mm, 5 mm, 8 mm, and 10 mm (see Fig. 7).

The variation of the above-listed parameters led to 24 different geometries of the proposed connections. Since three nominally identical specimens per varied geometry have been manufactured and tested, a total of seventy-two experimental tests were performed.

In order to easily distinguish each specimen and the relevant test results, the following identification code has been adopted: DC-Lα-tβ-dγ-#δ, where DC is for Ductile Connection, Lα for bonding width (e.g., L150 for the case of bonding width equal to 150 mm), tβ for the thickness of the web of the fuse (e.g., t5 corresponds to the case with thickness equal to 5 mm), dγ for the vertical pitch between holes of the fuse (e.g., d60 for the case with pitch equal to 60 mm), #δ for the number of repetitive tests performed per each configuration (e.g., #2 is the second test of the series of three nominally identical specimens).

The dimensions of all elements constituting the connection are summarized in Figs. 3-7. All steel and FRP elements were designed to be stronger than the channel fuse, but weaker than the adhesive moment resistance which was equal to about 5.4 kNm and 7.9 kNm for the bonding area equal to 150 mm x 150 mm and 150 mm x 220 mm, respectively. In this regard, the bonding moment resistance has been estimated in accordance with the formula proposed by Ascione et al. [35], namely as follows:

$$M = F \bullet d = \gamma \bullet \frac{1}{4} \bullet h^2 \bullet \sqrt{2 \bullet G_{II} \bullet E_{GFRP} \bullet t_{layer}} \tag{1}$$

where F is the vertical applied load at the free end of the beam at a distance d from the centroid of the adhesive layer whose height is h; G_{II} is the adhesive fracture energy in mode II; E_{GFRP} is the longitudinal Young modulus of the GFRP beam; t_{layer} is the thickness of the adhesive layer and γ is a correction factor that takes into account that the increase of the adhesive strength with the increase of the bonding width. The γ factor is derived as follows:

$$\gamma = \frac{b}{b_{eff}} \tag{2}$$

where b is bonding width and b_{eff} is optimal bonding width which is estimated on the basis of the Eq. (3):

$$b_{eff} = \frac{\pi}{2 \bullet \omega_s} ; \omega_s^2 = \frac{\beta_{II}}{E_{GFRP} \bullet t_{layer}} ; \beta_{II} = \tau_u / s_u \tag{3}$$

In Eq. (3), τ_u and s_u are the shear limit strength and ultimate slip of the adhesive, respectively.

The above-mentioned resistance values of the adhesive were obtained considering G_{II} equal to 4.10 N/mm, t_{layer} equal to 1 mm, E_{GFRP} equal to 24 GPa, h equal to 150 mm, d equal to 400 mm (bonding width of 150 mm) and equal to 365 mm (bonding width of 220 mm) as depicted in Fig. 9a. Assuming a bilinear constitutive behaviour for the adhesive, the estimated ultimate slip is 0.82 mm.

4.2. Materials

Araldite AV 5308 (Hardener HV 5309–1) [36] was used in this study as the adhesive material. This product is a bi-component epoxy adhesive produced by Huntsman Adv. Materials (Switzerland) and supplied by the Emanuele Mascherpa SpA (Italy). The main mechanical features of this structural adhesive are collected in Table 1. In particular, two of those were in the recent past [37] determined by experimental tests by

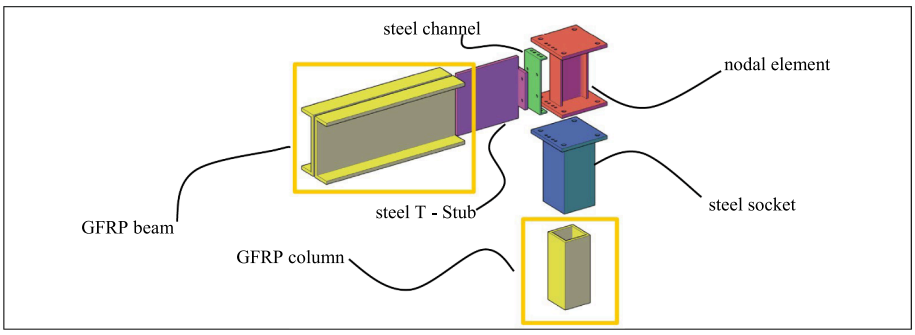

Fig. 1. The proposed hybrid connection and its main components.

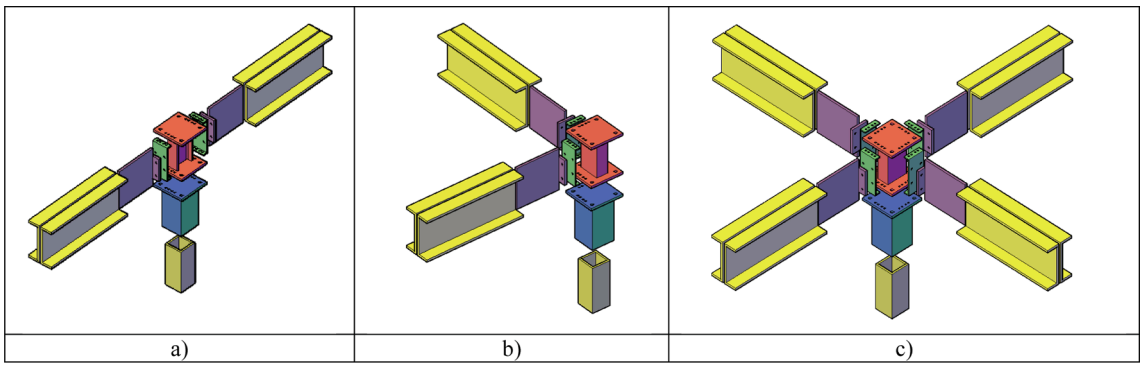

Fig. 2. The proposed hybrid connection for an internal 2D (a), corner 3D (b) and internal 3D (c) assembly.

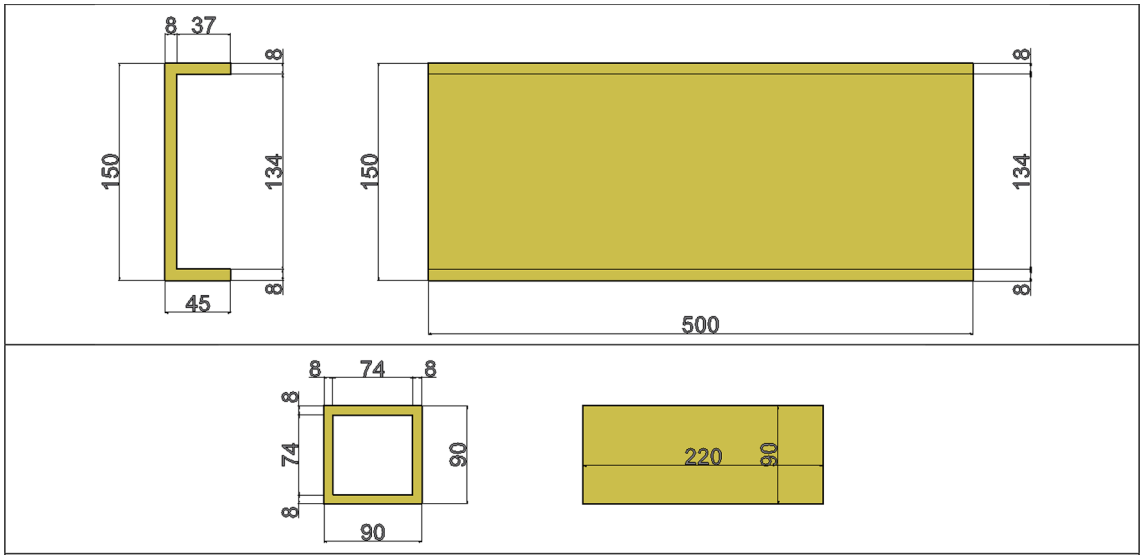

Fig. 3. Geometry of the GFRPs elements: channel profile for the beam and square hollow profile for the column.

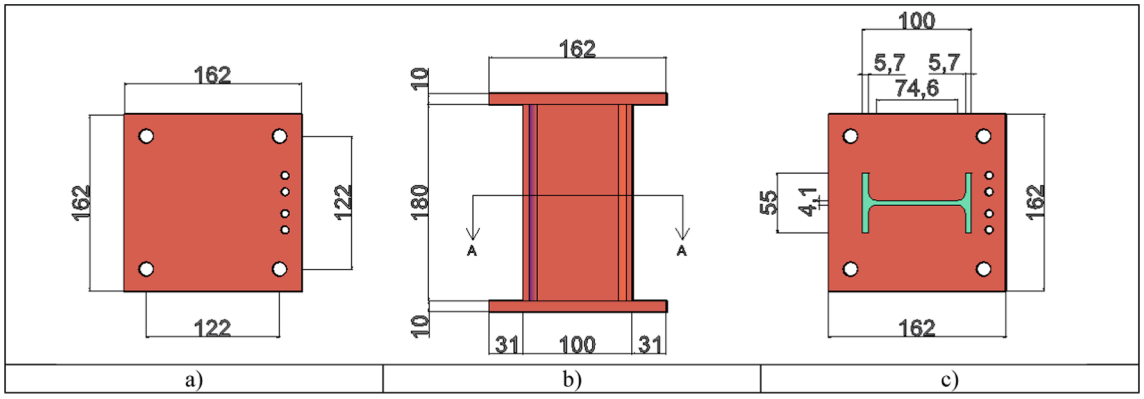

Fig. 4. Nodal element: a) end-plate (both topping and seating), b) I-profile, c) transverse section (A-A).

the authors: the glass transition temperature (T_g) and fracture energy in mode II, G_{II}. The first one was evaluated by Differential Scanning Calorimetry (DSC) test and ThermoGravimetric Analysis (TGA), while the second one by the Compliance-Based Beam Method (CBBM). The other properties were selected by the technical datasheet [36].

The Triglass® GFRP material used in this study is composed of a polyester matrix and glass fibres. The material was produced and supplied by Top Glass Industries S.p.A. (Italy) [38]. Its mean mechanical properties were derived from the datasheet provided by the supplier, and are summarized in Table 2.

The steel S275JR grade was selected for all steel elements, with a mean yield stress equal to 312 MPa and ultimate stress equal to 456 MPa (based on coupon tests performed on two specimens sampled from the channel representative of each thickness). Preloaded M12 bolts grade 10.9 were used, with ultimate stress equal to 1195 MPa.

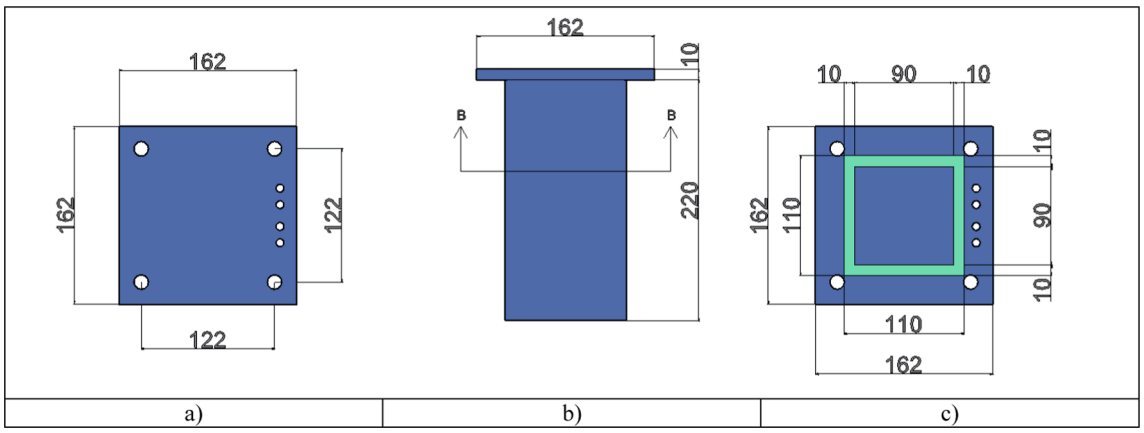

Fig. 5. Steel socket for column bonded connection: a) upper plate, b) socket, c) transverse section (B-B).

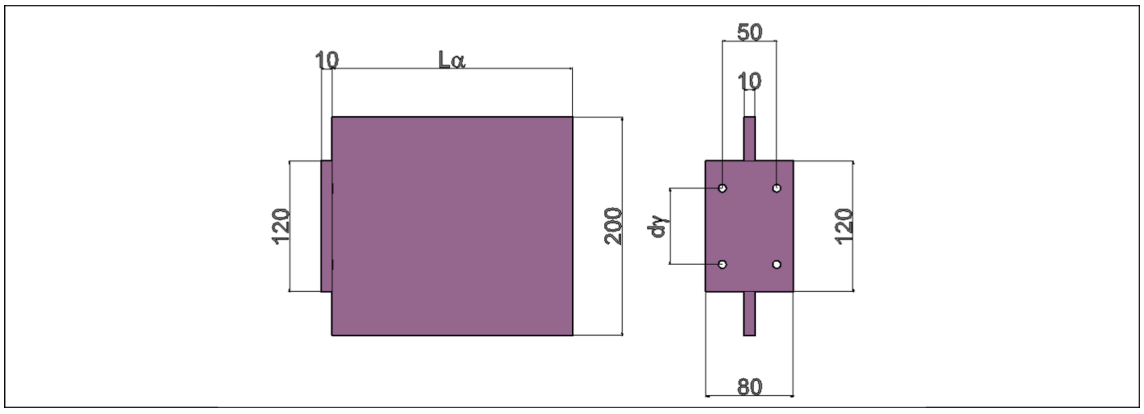

Fig. 6. Steel T-Stub to connect the GFRP beam to the fuse (Lα and dγ variable).

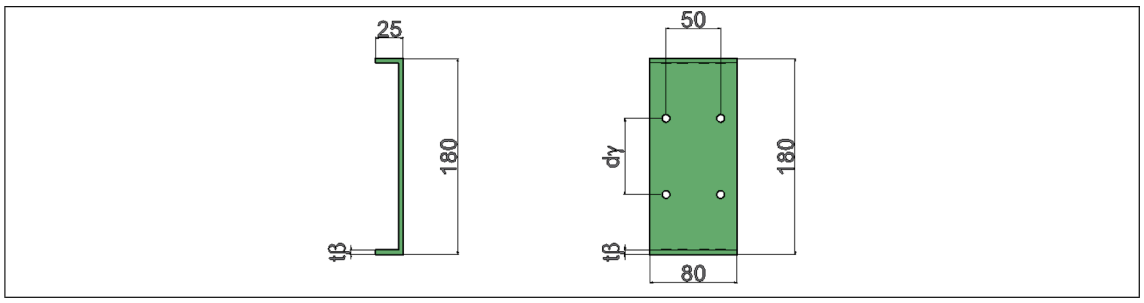

Fig. 7. Steel Fuse (tβ and dγ variable).

Table 1
Mechanical properties of the structural adhesive (Araldite AV 5308).

Density	T_g	Tensile Strength	Tensile Modulus	Shear Strength,τ_u	G_{II}
[g/cm^3]	[°C]	[MPa]	[GPa]	[MPa]	[N/mm]
1.40 (at 23 °C)	67	30 (at 23 °C)	2 (at 23 °C)	10 (at 23 °C)	4.10

4.3. Manufacturing of the specimens

The main manufacturing phases of each specimen are summarized in Fig. 8. In this regard, prior to the application of the adhesive, the surfaces of the bonded elements were prepared as follows: the steel surfaces were smoothed and GFRP elements were grit blasted, and then degreased with acetone (see Fig. 8a). Subsequently, the epoxy resin was prepared as shown in Fig. 8b, namely by considering a mixing weight ratio equal to 1:1. The components were mechanically mixed at a low speed of 500 rpm using a paddle mixer until uniform grey and neutral colours were achieved for the two systems. A spatula was used to check that there were no streaks near the bottom edges of the containers. The mixing was performed at room temperature (about 23 °C).

Afterwards, the bonded surfaces were glued as shown in Fig. 8c. It is worth highlighting that all specimens were glued in the same time interval in order to avoid any significant variations in the environmental condition as well as inconsistencies between the different adhesive mixtures. Furthermore, the bond-line thickness was nominally 1 mm. Spacers (calibrated steel bars of 1 mm) were inserted between the adherents before the application of the adhesive in order to control the

Table 2
Mechanical properties of the Triglass® material.

Property	Technical Standard used to evaluate the properties	Units	Mean values
Specific weight	ASTM D792	g/cm^3	1.75–1.90
Thermal class	–	CLASS	F
Coefficient of linear thermal expansion	ISO 11359–2	K^{-1}	8–11 x 10^{-6}
Thermal conductivity	EN 12,667 / EN 12664	W/mK	0.3
Longitudinal flexural strength	ASTM D790	MPa	300
Modulus of elasticity in longitudinal bending	EN 13,706	GPa	22 – 28
Modulus of elasticity with longitudinal traction	ASTIM D638	GPa	22 – 28
Elastic module with longitudinal compression	ASTM D695	GPa	16 – 20
Fire resistant	UL 94	CLASS	HB
Shear resistance	ASTM D2344	MPa	30

adhesive thickness. A similar procedure was adopted to glue the FRP column to the upper steel socket.

After having checked the alignment between the adherents by means of clamps, the specimens were cured for 24 h at room temperature.

Finally, Fig. 8d shows the specimen at the end of the curing process ready to be tested. As it can be observed, the FRP column is inserted into a steel tubular sleeve to restrain its flexural deformations.

4.4. Test set-up

All specimens were designed to simulate a sub-assemblage of an external corner beam-to-column joint. Therefore, the boundary and loading conditions were set accordingly. In fact, a monotonically increasing concentrated force was applied at the free tip of the beam by means of a rigid steel arm clamped to the upper part of the testing machine, which was a Schenck Hydropuls servo-hydraulic universal testing machine (Fig. 9).

As shown in Fig. 9a, the GFRP column was inserted into a steel jacket (internal free dimensions are 120 mm x 120 mm), which was clamped to the lower part of the testing machine.

The static tests were performed in displacement control at a rate of 2 mm/s.

In order to evaluate both the vertical displacement of the beam (at the same cross section where the load is applied) and the relative contribution of each part of the connection, linear variable displacement transducers (LVDT) were used (Fig. 9b) by Gefran (model PY-3 with a stoke of 100 mm and precision equal to 0.01).

Load cell data (PM-K with a nominal load of 630 kN and precision of 0.01 %) were automatically and continuously recorded by an automatic data acquisition system (System 5100 Vishay MM) with a frequency equal to 10 data per second.

5. Experimental results

The experimental response of the tested specimens is shown in terms of force–displacement (F-δ) and moment-rotation (M-φ) curves (three per tested configuration) in Figs. 10 and 11, respectively. The force F is the force applied at the tip of the beam; the moment M is evaluated at the web of the structural fuse (which corresponds to a lever arm equal to 475 mm, see Fig. 9a). The displacement δ is evaluated at the free end of the beam and the rotation φ is the overall chord rotation, namely the displacement δ divided by the free length of the cantilever beam (i.e., 475 mm).

The main mechanical parameters of the experimental curves are evaluated on the basis of Fig. 12. In fact, the elastic stiffness (K_{el}) is equal to the ratio (M_{el}/φ_{el}), where φ_{el} is the rotation corresponding to elastic resistance. The threshold of the elastic moment M_{el} is evaluated on the basis of the ECCS-45 procedure [39] as depicted in Figs. 10 and 11, namely as the intersection between the elastic stiffness and the tangent post-yielding stiffness, the latter having slope (K_p) equal to (K_{el}/10). All experimentally measured values are summarized in Tables 3-6. The values of M_{el}, which correspond to the plastic resistance of the steel fuse whose typical damage pattern is depicted in Fig. 13, are lower than the adhesive resistance (see Section 4.1).

From observation of the experimental damage patterns, the response curves and the data summarised in Tables 3-6, it can be concluded that:

- The resistance and stiffness of the joint are strongly influenced by

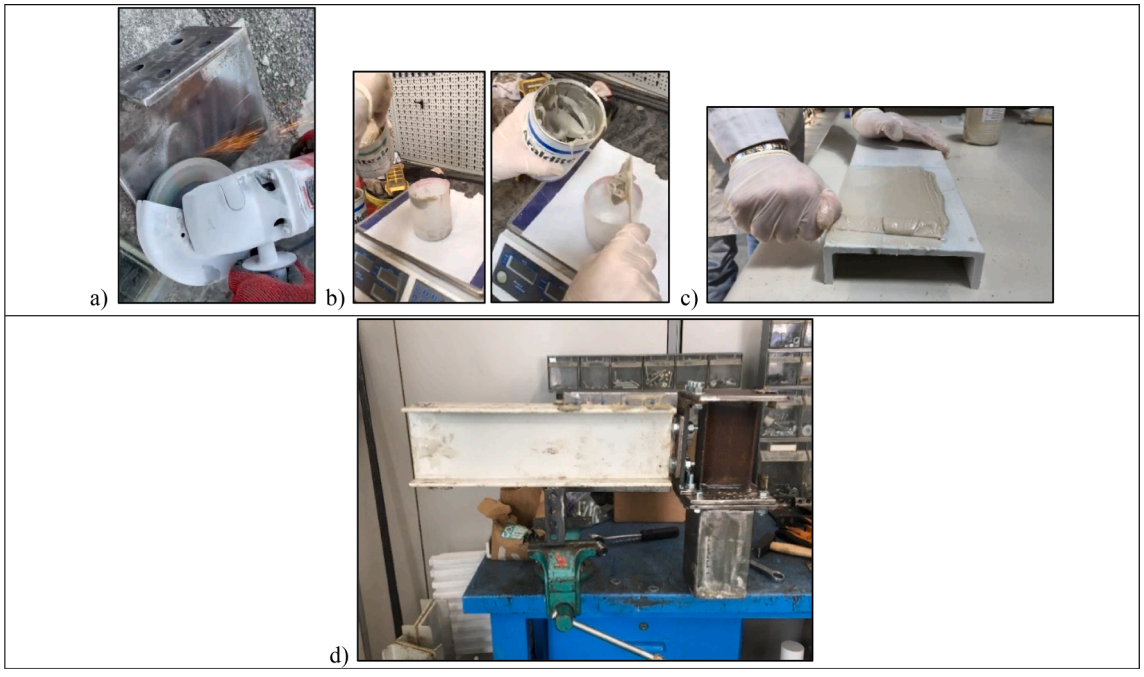

Fig. 8. Manufacturing of the specimens: (a) preparation of the surfaces of the bonded elements; (b) epoxy resin preparation; (c) glueing process; (d) assembled specimen.

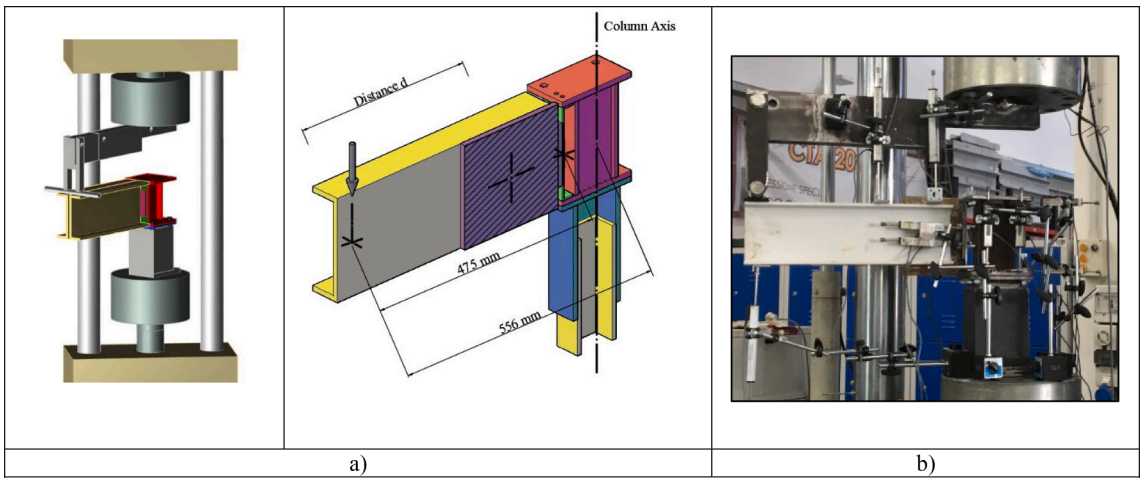

Fig. 9. Test set-up: a) schematic 3D views; b) c) the specimen ready to be tested.

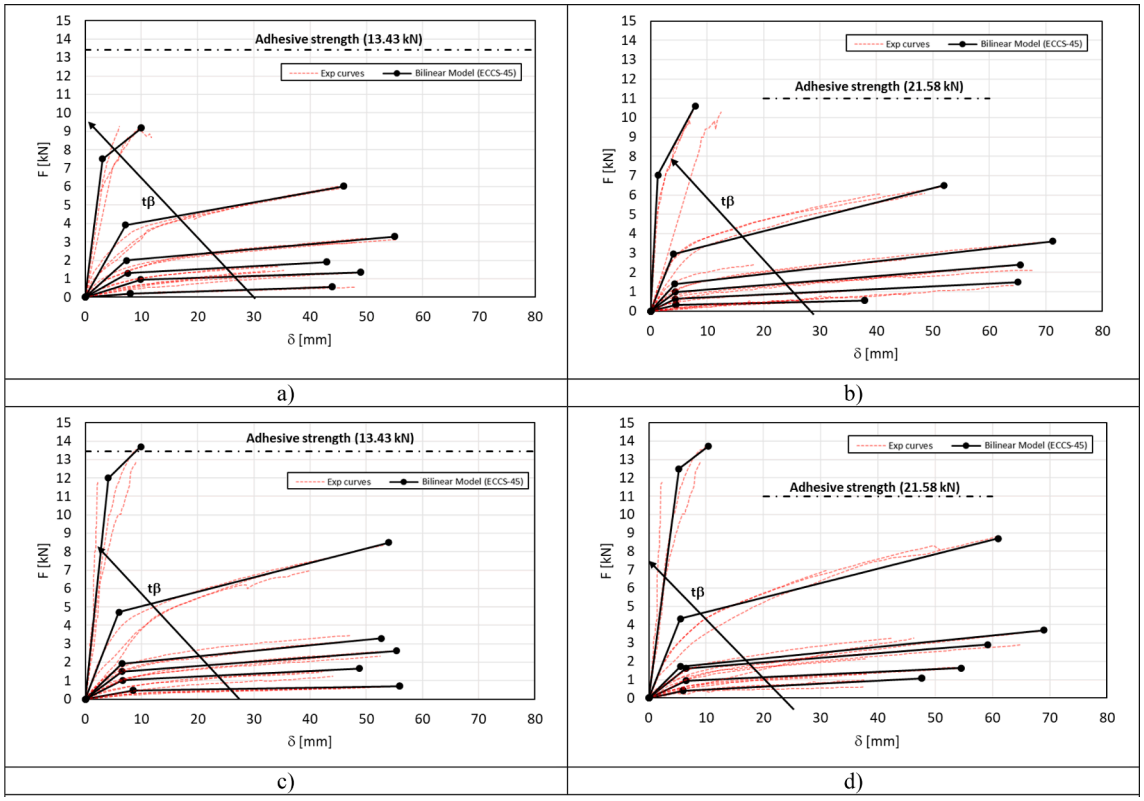

Fig. 10. Experimental force–displacement curves: a) DC-L150-d60, b) DC-L220-d60, c) DC-L150-d80, d) DC-L220-d80.

the thickness of the web of the steel fuse. It is rather trivial to realise that the thicker the web of the fuse, the stiffer and stronger the joint, although the ductility decreases. This result depends directly on the bending behaviour of the steel joint, the resistance and rigidity of which depend on the cross section of the web plate;

- If the pitch of the bolts clamping the fuse and the T-Stub is the same, but the width of the joint varies, the stiffness of the joint increases with the width of the joint.

However, this result is mainly due to the size of the samples. In fact, the length of the beam is rather small (length to depth ratio equal to 3.54). Therefore, the bond length corresponds to a rigid offset, the effect of which is more sensitive in short span beams. It is expected that such an effect will be negligible for cases with longer spans (e.g. length to depth ratio from 5 to 10);

- For the same bond width, but varying the pitch of the bolts clamping the fuse and the T-Stub, the resistance and rigidity of the joint were significantly affected. The greater the pitch, the greater the resistance and stiffness of the joint. This effect depends on the lever arm of the joint, which is also associated with a more efficient distribution of the linear yield lines that develop in the web of the fuse, which occur close to the bolt rows.

6. The proposed connection vs. other types: comparison of mechanical performances

In order to assess the effectiveness of the proposed connections, their mechanical response has been compared against those of the connections that have been described and discussed in the literature review of

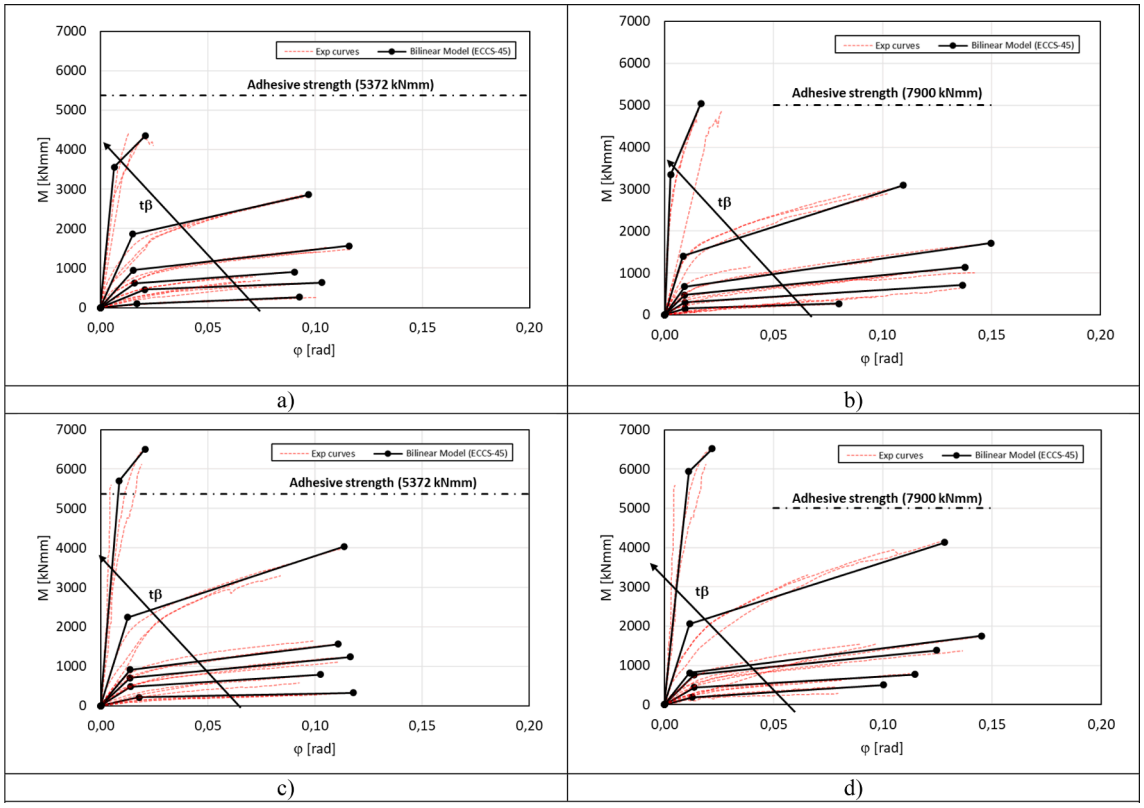

Fig. 11. Experimental moment-rotation curves: a) DC-L150-d60, b) DC-L220-d60, c) DC-L150-d80, d) DC-L220-d80.

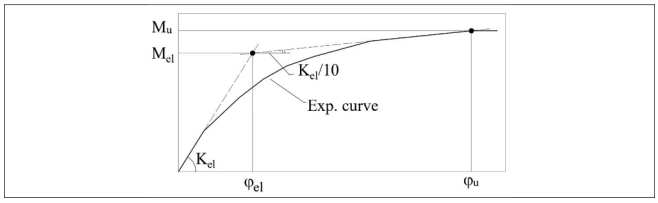

Fig. 12. Graphical procedure to evaluate the elastic resistance of the connection.

Table 3
Bilinear values for DC-L150-d60 series.

fuse web thickness	M_{el} [kNmm]	φ_{el} [rad]	K_{el} [kNmm/rad]
2	95,000	0,017	5,571E + 03
3	456,000	0,021	2,191E + 04
4	618,925	0,016	3,868E + 04
5	949,550	0,015	6,157E + 04
8	1861,050	0,015	1,228E + 05
10	3562,500	0,007	5,460E + 05

Table 4
Bilinear values for DC-L150-d80 series.

fuse web thickness	M_{el} [kNmm]	φ_{el} [rad]	K_{el} [kNmm/rad]
2	213,750	0,018	1,194E + 04
3	484,500	0,014	3,487E + 04
4	712,500	0,014	5,174E + 04
5	916,275	0,014	6,696E + 04
8	2243,425	0,013	1,776E + 05
10	5700,000	0,009	6,613E + 05

Table 5
Bilinear values for DC-L220-d60 series.

fuse web thickness	M_{el} [kNmm]	φ_{el} [rad]	K_{el} [kNmm/rad]
2	152,475	0,009	1,609E + 04
3	299,725	0,009	3,236E + 04
4	475,000	0,009	5,168E + 04
5	670,700	0,009	7,409E + 04
8	1403,625	0,008	1,667E + 05
10	3342,575	0,003	1,221E + 06

Table 6
Bilinear values for DC-L220-d80 series.

fuse web thickness	M_{el} [kNmm]	φ_{el} [rad]	K_{el} [kNmm/rad]
2	190,000	0,013	1,504E + 04
3	445,313	0,014	3,254E + 04
4	763,800	0,014	5,582E + 04
5	815,813	0,012	7,046E + 04
8	2056,750	0,012	1,776E + 05
10	5937,500	0,011	5,369E + 05

Section 2. For the sake of comparison, both resistances and ultimate rotations have been normalized as follows: (i) the normalized resistance (η) has been computed as the ratio between the ultimate moment (M_u) and the moment capacity of the beam (M_b); the ultimate rotation (ϕ_u) has been normalized to the elastic one (ϕ_{el}), thus providing the measure of the connection ductility (μ).

Table 7 summarizes the mechanical parameters of each type of considered connection, where from the left to the right columns the reader can find: the reference number of the considered experimental study; the type of connection (Bolted, Adhesive, Hybrid); the shapes of the beam, the column, and the reinforcement (if present); the resistance

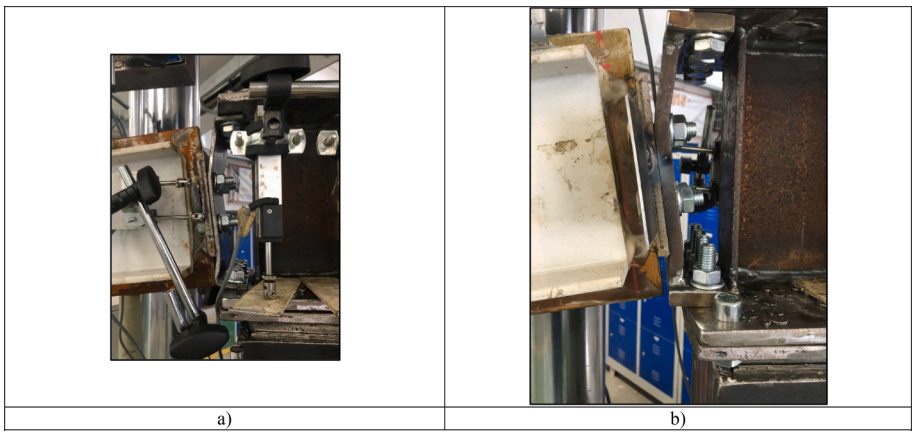

Fig. 13. Some examples of damage patterns in the steel fuse: a) DC-L150-d60-t3, b) DC-L220-d60-t10.

modulus (W_b) in the major axis of the beam; the ultimate stress (σ_u) of the pultruded profiles; the experimental elastic moment (M_{el}) of the connection; its corresponding elastic rotation (ϕ_{el}); the ultimate moment (M_u); its corresponding rotation (ϕ_u); the Navier flexural resistance of the pultruded beam (M_b); the normalized resistance (η); the ductility (μ); the type of failure mode.

The normalised resistance and associated ductility of these joints are also compared in Fig. 14 where adhesive joints are identified by a full circle, all bolted joints by a square and all hybrid joints by a triangle. In addition, the results for the proposed joint are indicated by a circle.

Bolted joints.

It can be seen that, on average, bolted joints show good ductility, but their average resistance is rather low compared to the other types of joints. In fact, the holes in the FRP are responsible for a premature loss of resistance; therefore, these joints cannot take advantage of the superior resistance of the FRP.

Adhesive joints.

On the contrary, bonded joints can have greater resistance and stiffness due to the continuity of the fibres and the almost uniform diffusion of the stress state in the adhesive layer. This is confirmed by the high values of the parameter η for the adhesive companion joints. However, due to their brittle failure, the fully bonded joints cannot exhibit any ductility (the parameter μ is equal to one). Therefore, they are not allowed [40].

Hybrid joints.

On average, the hybrid joints studied are stronger and more ductile than the fully bolted and bonded joints. In particular, they are characterised by a level of resistance and stiffness due to the adhesive layer, while the presence of steel parts is only necessary to prevent the collapse of the system (plastic reserve).

Proposed hybrid joint.

As expected, the proposed hybrid joint exhibits different levels of resistance and ductility. The result shown in Fig. 14 (full circle) is relative to the strongest joint tested by the authors, which is the specimen identified as DC-L220-t10-d80. This type of joint is characterised by the greatest width of the adhesive layer (220 mm), the greatest vertical distance between the bolts (80 mm) and the thickest web of the fuse.

Its resistance ($\eta = 16$ %) is lower than that of any other fully bonded joint (where failure typically starts in the adhesive), but comparable and/or higher than that of the bolted joints discussed. In fact, the proposed joint is deliberately designed to be weaker than the adhesive strength to avoid adhesive collapse, but for ensuring such a behaviour the resistance of the joint is penalized.

To increase the resistance of the proposed joint, it seems feasible to increase the height of the adhesive area. In fact, as shown by Ascione et al. in [35], the resistance of the adhesive layers is determined by the branch between the resultants of the tangential stresses due to torsion (aligned along the beam axis). The latter consideration is also supported by Eq. (1), where the adhesive torsional resistance M depends quadratically on the height h of the adhesive area.

In terms of ductility, the proposed joint shows values (μ ranging of 2 and 17) that are significantly higher than those of all the joints considered. The results shown in Fig. 14 (circles) correspond to the DC-L220-d60 specimens with parameter t ranging from 2 to 10 mm. According to Fig. 14, the strongest joints are those with the greatest bond width (i.e. 220 mm) and the smallest vertical distance between the bolts (i.e. 60 mm). Therefore, the higher the bond width, the higher the resistance and ductility of the proposed joint, while the lower the bolt spacing, the higher the ductility (but not the resistance). Furthermore, as expected, the higher values of the dimensionless parameter μ were found for intermediate values of t (3, 4, 5 and 8 mm). The extreme values (2 and 10 mm) resulted in lower ductilities due to the following problems: for t equal to 2 mm, the ductility was penalised by excessive deformability (see Fig. 13a) and low resistance of the system; for t equal to 10 mm, the ductility was penalized by the high stiffness of the system.

The elastic stiffness comparison is shown in Fig. 15. The vertical axis shows the ratio between the experimental moment and the Navier bending resistance of the beam. It can be seen that the stiffness of the proposed joint is higher than most of the bolted and hybrid joints considered, but obviously lower than the adhesive joints.

In general, it can be said that the proposed hybrid joints showed satisfactory resistance and ductility. However, unlike the other types compared in Table 7, the damage is concentrated only in the steel part, which allows to protect the integrity of the adhesive layers and the GFRP elements (reuse of GFRP structures), as well as to facilitate the repair of the assembly by simply replacing the yielded steel parts. This last aspect is considered very promising for the practical use of the proposed joints.

7. Conclusion and future developments

This paper describes the results of an extensive experimental investigation carried out with the aim of developing a novel ductile hybrid beam to column connection for FRP structures. The proposed type of connection has recently been patented and is designed to overcome the main criticisms of bolted and bonded connections, namely the low resistance and rigidity of bolted connections and the brittle response of bonded connections. The main novelty of the proposed hybrid connection is the idea of using a steel component of the connection specifically designed as a structural fuse, namely the weaker part of the beam-column assembly, while the remaining elements are designed to remain in the elastic range.

An extensive experimental program has been carried out and the results obtained allow the following observations to be made:

Table 7
Comparison with similar connections available in the literature.

Reference	Type of Connection	Cross section of the profiles	W_b	σ_u	M_{el}	φ_{el}	M_u	φ_u	M_b	η	μ	Failure mode
[#]	[#]	[#]	[cm^3]	[MPa]	[kNm]	[mrad]	[kNm]	[mrad]	[kNm]	[%]	[-]	[#]
[4]	Bolted	Beam: I Column: I Reinforc.: L	405	317	0.7	0.80	1.4	2.20	128.6	1.1	2.8	Flange column delamination
[10]	Bolted	Beam: Box Column: Box Reinforc.: ideal. Bolted steel cuff	37	138	–	–	6.5	–	5.0	128.9	–	Web-flange column separation
[13]	Bolted	Beam: I Column: I Reinforc.: L	651	228	0.5	3.90	2.0	34.00	148.1	1.3	8.7	Seat angle delamination
[15]	Bolted	Beam: Box Column: Box Reinforc.: Steel box	149	415	4.0	50.00	6.0	210.00	61.9	9.7	4.2	Bearing
[17]	Bolted	Beam: Box Column: Steel Reinforc.: Bolted sleeve box	15	230	0.25	10.00	2.8	100.00	3.4	81.8	10.0	Web-flange beam separation
[18]	Bolted	Beam: Box Column: Box Reinforc.: Bolted steel cuff	149	294	4.3	40.00	8.0	250.00	41.9	19.0	6.3	Cuff local cracks GFRP Bearing
[19]	Bolted	Beam: I Column: I Reinforc.: Bolted steel cuff	102	371	4.0	32.82	6.1	84.16	37.9	16.1	2.6	Web-flange column separation
[20]	Bolted	Beam: I Column: I Reinforc.: L	102	359	3.0	13.72	7.1	165.27	36.6	19.4	12.0	Column Local cracks
[23]	Adhesive	Beam: Box Column: Box Reinforc.: adhesive Cuff	37	207	7.5	4.00	7.5	4.00	7.6	99.2	1.0	Adhesive
[24]	Adhesive	Beam: Box Column: Box Reinforc.: adhesive Cuff	37	207	10	10.00	10	10.00	7.6	132.2	1.0	Cuff local cracks
[25]	Adhesive	Beam: I Column: I Reinforc.: L	229	240	10.2	25.00	10.2	25.00	55.0	18.4	1.0	Adhesive/ delamination
[26]	Adhesive	Beam: U (built-up) Column: Box Reinforc.: L	142	240	11.3	60.00	11.3	60.00	34.1	33.1	1.0	Adhesive
[27]	Adhesive	Beam: U (built-up) Column: Box Reinforc.: L	140	300	6.5	68.00	6.5	68.00	42.0	15.5	1.0	Adhesive
[29]	Hybrid	Beam: Box Column: Steel	99	230	8.5	8.37	15.5	34.89*	22.8	67.9	4.2	Web-flange beam separation
[30]	Hybrid	Beam: Box Column: Box	99	307	4.0	11.00	7.1	40.00	30.5	23.2	3.6	Web-flange beam separation
[32]	Hybrid	Beam: U (built-up) Column: Box	1132	554	44.0	12.66	65.0	83.33	626.8	10.4	6.6	Adhesive/bearing
P.C. DC L220-t10-d80	Hybrid	Beam: U (built-up) Column: Box	140	300	5.9	11.06	6.5	21.85	42.0	15.6	2.0	Steel yielding
P.C. DC L220-t2-d60	Hybrid	Beam: U (built-up) Column: Box	140	300	0.2	9.47	0.3	80.00	42.0	0.6	8.4	Steel yielding
P.C. DC L220-t3-d60	Hybrid	Beam: U (built-up) Column: Box	140	300	0.3	9.26	0.7	136.84	42.0	1.7	14.8	Steel yielding
P.C. DC L220-t4-d60	Hybrid	Beam: U (built-up) Column: Box	140	300	0.5	9.19	1.1	137.87	42.0	2.7	15.0	Steel yielding
P.C. DC L220-t5-d60	Hybrid	Beam: U (built-up) Column: Box	140	300	0.7	9.05	1.7	149.92	42.0	4.1	16.6	Steel yielding
P.C. DC L220-t8-d60	Hybrid	Beam: U (built-up) Column: Box	140	300	1.4	8.42	3.1	109.47	42.0	7.4	13.0	Steel yielding
P.C. DC L220-t10-d60	Hybrid	Beam: U (built-up) Column: Box	140	300	3.3	2.74	5.0	16.63	42.0	12.0	6.1	Steel yielding

– The thickness of the structural fuse has a significant effect on the resistance and stiffness of the joint;
– Varying the bond width between the FRP beams and the steel connectors influences the rigidity of the beam-column assembly because the bonded part of the beam behaves as a rigid end offset;
– Varying the pitch of the bolts of the structural fuse affects the resistance and rigidity of the connections.

Further numerical and analytical studies are considered necessary to investigate the local response of each component of the proposed

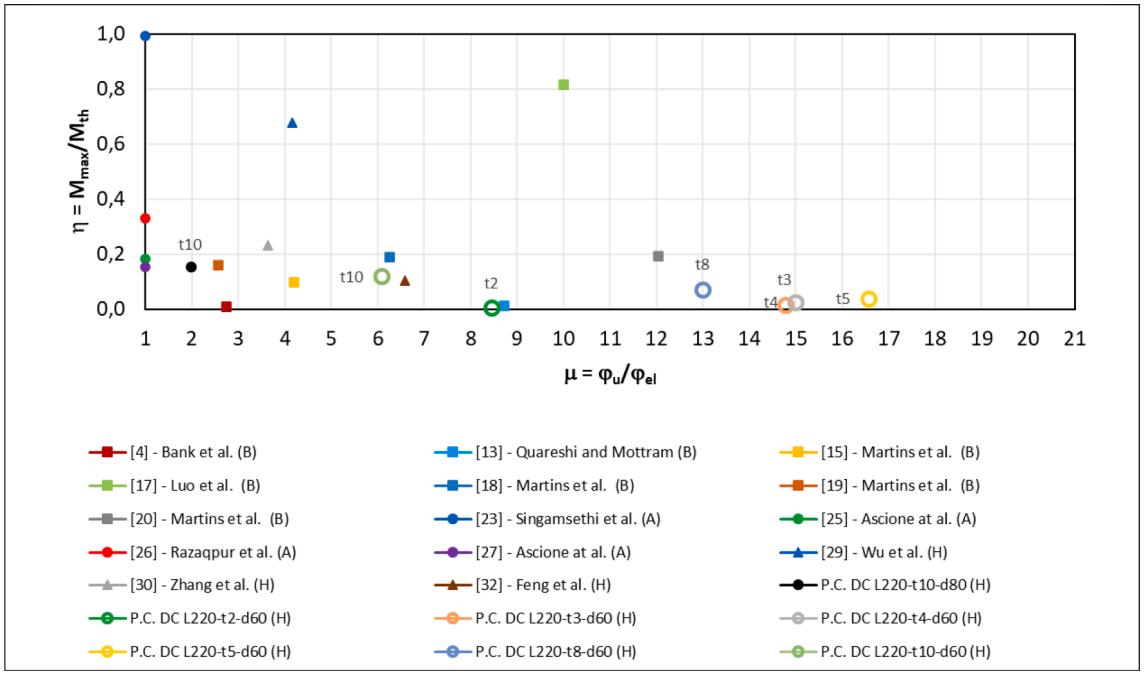

Fig. 14. Comparison of the mechanical performance.

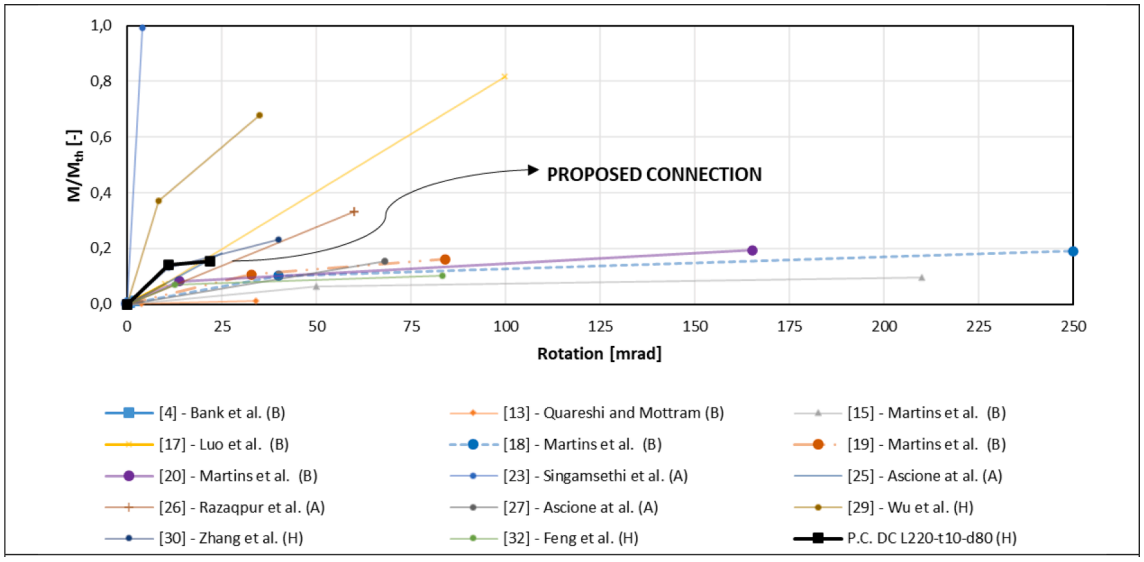

Fig. 15. Comparison of the elastic stiffness.

connection and to develop equations for easy use and effective design of the proposed connection.

CRediT authorship contribution statement

Francesco Ascione: Writing – review & editing, Writing – original draft, Visualization, Validation, Supervision, Methodology, Investigation, Data curation, Conceptualization. **Mario D'Aniello:** Writing – review & editing, Writing – original draft, Visualization, Methodology, Investigation, Conceptualization. **Luciano Feo:** Writing – review & editing, Visualization, Supervision, Methodology, Conceptualization. **Luigi Granata:** Writing – original draft, Validation, Resources, Methodology, Investigation, Formal analysis, Data curation. **Raffaele Landolfo:** Writing – review & editing, Visualization, Supervision, Methodology, Conceptualization.

Declaration of competing interest

The authors declare that they have no known competing financial interests or personal relationships that could have appeared to influence the work reported in this paper.

Data availability

No data was used for the research described in the article.

Acknowledgements

The Authors gratefully acknowledge: 1) Emanuele Mascherpa SpA, for supplying the Araldite AV 5308; 2) Top Glass Industries S.p.A. (Italy) for providing the G-FRP profiles.

References

[1] Mosallam, A.S. Design guide for FRP composite connections. Manuals of practice (MOP) 102. American Society of Civil Engineers (ASCE).
[2] Zhu Y, Fascetti A, Feo L, Mosallam AS, Penna R. Experimental and Numerical Characterization of PFRP structural elements with stiffened web-flange junctions. Compos Struct 2022;116383.
[3] Quadrino A, Penna R, Feo L, Nisticò N. Mechanical characterization of pultruded elements: fiber orientation influence vs web-flange junction local problem. Experimental and numerical tests Comp Part B 2018;142:68–84.
[4] Bank LC, Mosallam AS, Gonsoir HE. Beam-to-column connections for pultruded FRP structures. In: Suprenant B, editor. Serviceability and durability of construction materials. Proceedings of the first materials engineering congress, Denver, CO, 13–15 August, ASCE; 1990. p. 804–13.
[5] Bank LC, Mosallam AS, McCoy GT. Design and performance of connections for pultruded frame structures. Reinf Plast Compos 1994;15:1052–67.
[6] Mosallam AS. Stiffness and strength characteristics of PFRP UC/beam-to- column connections. In: Composite material technology, PD-vol.53, Proceedings, ASME Energy-Sources Technology Conference and Expo, TX, 331 January-4 February; 1993. p. 275–83.
[7] Mosallam AS, Abdelhamid MK, Conway JH. Performance of pultruded FRP connections under static and dynamic loads. J Reinf Plast Compos 1994;13: 386–407.
[8] Bank LC, Yin J, Moore L. Experimental and numerical evaluation of beam-to-column connections for pultruded structures. J Reinf Plast Compos 1996;15: 1052–67.
[9] Smith SJ, Parsons ID, Hjelmstad KD. An experimental study of the behaviour of connections for pultruded GFRP I-beams and rectangular tubes. J Compos Constr 1998;42:281–90.
[10] Smith SJ, Parsons ID, Hjelmstad KD. Experimental comparisons of connections for GFRP pultruded frames. J Compos Constr 1999;3:20–6.
[11] Qureshi J, Mottram JT. Behaviour of pultruded beam-to-column joints using steel web cleats. Thin-Walled Struct 2013;73:48–56.
[12] Qureshi J, Mottram JT. Response of beam-to-column web cleated joints for FRP pultruded members. J Compos Constr 2014;18.
[13] Qureshi J, Mottram JT. Moment-rotation response of nominally pinned beam-to-column joints for frames of pultruded fibre reinforced polymer. Constr Build Mater 2015;77:396–403.
[14] Clarke JL. Structural design of polymer composites: EUROCOMP design code and handbook. London: E & FN Spon; 1996.
[15] Martins D, Correia JR, Gonilha J, Arruda M, Silvestre N. Development of a novel beam-to-column connection system for pultruded GFRP tubular profiles. Compos Struct 2017;171:263–76.
[16] Russo S. On failure modes and design of multi-bolted FRP plate in structural joints. Compos Struct 2019;218:27–39.
[17] Luo FJ, Huang Y, He X, Qi Y, Bai Y. Development of latticed structures with bolted steel sleeve and plate connection and hollow section GFRP members. Thin-Walled Struct 2019;137:106–16.
[18] Martins D, Gonilha J, Correia JR, Silvestre N. Monotonic and cyclic behaviour of cuff beam-to-column connection system for tubular pultruded GFRP profiles. Eng Struct 2021;247:113165.
[19] Martins D, Gonilha J, Correia JR, Silvestre N. Monotonic and cyclic behaviour of a stainless steel cuff system for beam-to-column connections between pultruded I-section GFRP profiles. Eng Struct 2021;249:113294.
[20] Martins D, Gonilha J, Correia JR, Silvestre N. Exterior beam-to-column bolted connections between GFRP I-shaped pultruded profiles using stainless steel cleats. Part 1: Experimental study. Thin-Walled Struct 2021;163:107719.
[21] Martins D, Gonilha J, Correia JR, Silvestre N. Exterior beam-to-column bolted connections between GFRP I-shaped pultruded profiles using stainless steel cleats, Part 2: prediction of initial stiffness and strength. Thin-Walled Struct 2021;164: 107762.
[22] Ferrara G, Helson O, Michel L, Ferrier E. Mechanical Characterisation of GFRP frame and beam-to-column joints including steel plate fastened connections. Materials 2022;15:8282. https://doi.org/10.3390/ma15238282.
[23] Singamsethi S, LaFave J, Hjelmstad K. Fabrication and testing of cuff connections for GFRP box sections. J Compos Constr 2005;9(6):536–44.
[24] Carrion JE, LaFave J, Hjelmstad K. Experimental behavior of monolithic composite cuff connections for fiber reinforced plastic box sections, 2005.
[25] Ascione F, Lamberti M, Razaqpur AG, Spadea S. Strength and stiffness of adhesively bonded GFRP beam-column moment resisting connections. Compos Struct 2017;160:1248–57.
[26] Razaqpur AG, Ascione F, Lamberti M, Spadea S, Malagic M. GFRP hollow column to built-up beam adhesive connection: mechanical behaviour under quasi-static, cyclic and fatigue loading. Compos Struct 2019;224:111069.
[27] Ascione F, Granata L, Carozzi G. Flexural and shear behaviour of adhesive connections for large scale GFRP frames: influence of the bonded area and hygrothermal aging. Compos Struct 2023;283:115122.
[28] Zhang Z, Wu C, Nie X, Bai Y, Zhu L. Bonded sleeve connections for joining tubular GFRP beam to steel member: Numerical investigation with experimental validation. Compos Struct 2016;157:51–61.
[29] Wu C, Zhang Z, Bai Y. Connections of tubular GFRP wall studs to steel beams for building. Construction Comp part B 2016;95:64–75.
[30] Zhang ZJ, Bai Y, Xiao X. Bonded sleeve connections for joining Tubular glass fiber-reinforced Polymer beams and columns. Experimental and Numerical Studies 2018.
[31] Qiu C, Bai Y, Zhang L, Jin L. Bending performance of splice connections for assembly of Tubular section FRP members: Experimental and Numerical study. J Compos Constr 2019;23(5).
[32] Feng P. Quasi-plastic flexural behavior of adhesive-bolt hybrid connection for large scale pultruded GFRP frame. Eng Struct 2021;238:112200.
[33] Feo L, Latour M, Penna R, Rizzano G. Pilot study on the experimental behavior of gfrp-steel slip-critical connections. Comp Part B 2017;115:209–22.
[34] Industrial Patent for “Dissipative connection for fiber reinforced elements”, n. 102023000005838, presented on 27th of March 2023 by the University of Salerno (inventors Ascione F, D’Aniello M, Feo L, Granata L, Landolfo R.).
[35] Ascione F, Granata L. Mechanical models for predicting the strength and stiffness of a beam-to-column adhesively-bonded connection between pultruded profiles. Structures 2022;43:493–507.
[36] Araldite technical data sheet; 2020 - huntsman.com.
[37] Ascione F, Granata L, Guadagno L, Naddeo C. Hygrothermal durability of epoxy adhesives used in civil structural applications. Compos Struct 2021;265:113591.
[38] Top Glass Industries S.p.A; www.topglass.it.
[39] Eccs-45 - European convention for constructional steelwork, recommended testing procedure for assessing the behaviour of steel elements under cyclic loads 1986 Brussels.
[40] CEN/TS 19101: 2022. Design of fibre-polymer composite structures.